Received: 29 April 2025 | Revised: 14 November 2025 | Accepted: 16 November 2025

DOI: 10.5185/amlett.2026.011779

OPEN ACCESS

RESEARCH

Investigation of Doping Effects and Defects in Chiral Carbon Nanotubes

Thaizy C. Nossa[1,2]*, Paulo José Pereira de Oliveira[3]*

[1]Department of Physics, Federal University of Ouro Preto (UFOP) - Morro do Cruzeiro unit, Minas Gerais, 35400-000, Brazil

[2]Federal Institute of Education, Science and Technology of Espírito Santo – Unit Cariacica City, 29150-410, Brazil

[3]Federal Institute of Education, Science and Technology of Espírito Santo – Unit Cachoeiro de Itapemirim City, P.O. Box 727, 29311-970, Brazil

***Corresponding author:**

E-mail:
thaizy.nossa@aluno.ufop.edu.br
paulojoseo@ifes.edu.br

ABSTRACT

Carbon nanotubes are allotropes of carbon and are 1D nanomaterials with various applications, including their use as sensors, in composites, and even as drug delivery vectors. In this study, we employed density functional theory with a local density approximation, implemented in the SIESTA software, to analyze the electrical properties of the chiral (6,3) carbon nanotube containing 48 carbon atoms. We performed studies on energy bands and total and partial density of states. Systems doped with Boron and Nitrogen were investigated, as well as simulations of defects (vacancies). Our results indicate that the nanotube exhibits semiconducting behavior with a bandgap of 0.115 eV. However, after the inclusion of Nitrogen, Boron, and vacancy impurities, its character changes to metallic, with energy bands crossing the Fermi level. The density of states analysis revealed that the carbon 2p orbitals contribute the most to charge mobility compared to the 2p orbitals of Boron and Nitrogen, and also when vacancies are included.

KEYWORDS

Chiral Nanotube, DFT, Doping, band gap

INTRODUCTION

Interestingly, nanoscience and nanotechnology developed alongside the discovery of a new class of materials that are allotropic forms of carbon with great potential for technological applications, as in the case of Carbon Nanotubes (CNTs) [**1**]. CNTs consist of hexagonally arranged carbon atoms forming cylindrical nanostructures. Their diameters typically range from a few angstroms to several tens of nanometers, while their lengths can extend to several centimeters [**2**]. Single-walled carbon nanotubes (SWNTs) are nanomaterials with broad potential for applications across interdisciplinary fields, integrating physics, chemistry, and biology [**3**]. The properties of carbon nanotubes (CNTs) are directly influenced by their diameter and chirality. The manner in which the graphene sheet is rolled determines their structure and, consequently, their electronic properties. CNTs are classified as zigzag, armchair, or chiral, and can exhibit either metallic or semiconducting behaviour [**4**]. The manipulation of the electronic properties of carbon nanotubes can be achieved through doping, substituting carbon atoms with other chemical species such as boron or nitrogen or by introducing topological defects into the hexagonal lattice [**5**]. Doping with heteroatoms is an effective approach for tuning the structural and electronic properties of carbon nanotubes [**6**]. Nitrogen (**N**) doping, for instance, can induce negative charge localization on adjacent carbon atoms, thereby increasing the electrode's capacitance. This makes N-doped CNTs highly suitable materials for supercapacitor applications [**7,8,9**]. In this work, single-walled carbon nanotubes (SWCNTs) composed of 48 carbon atoms were studied, specifically of the chiral type, which are asymmetric, with the aim of computationally investigating the behavior of their physical and chemical properties in the presence of impurities and defects. In addition to the diameter, chirality is a key factor influencing the electronic properties of nanotubes. The chirality of carbon nanotubes is indicated by the chiral indices (also known as Hamada indices) represented by (n, m). When $n = 0$ and $m \neq 0$, the nanotube is of the zigzag type, when $n = m$, the nanotube is of the armchair type, and for other combinations of n and m the nanotube is classified as chiral. In the present work, we present a computational study of the electrical properties and chemical analysis of a doped chiral-type nanotube with defects. In the literature, we find few studies involving chiral-type nanotubes compared to research on armchair and zigzag nanotubes, which motivated us to carry out this study.

COMPUTATIONAL METHODOLOGY

The initial nanotube structure was of the chiral type with Hamada indices (6,3), consisting of 48 carbon atoms (CNT-48C). The nanotube was constructed using the Nanotube Modeler software [**10**].

Calculations were performed using the Density Functional Theory (DFT) method, employing the Local Density Approximation (LDA) with CA parameterization as the exchange-correlation functional. The pseudopotentials required for the calculations can be obtained from reference [**11**]. We chose this database because its pseudopotentials have shown good agreement with previous literature in DFT studies of carbon nanotubes using the LDA approximation [**12-13**]. A kinetic energy cutoff of 300 Ry was used for the plane waves, and the following symmetry points were considered for the construction of the energy bands: Γ (0, 0, 0) and X (0, 0, 1). These points are given in units of the reciprocal lattice vectors, with a unit cell constant of 7.0 Å, considering a unit cell with dimensions a = b = 21 Å and c = 7.0 Å, and angles α = β = γ = 90°. Larger values for the a and b parameters were adopted to minimize mirror interactions in these directions due to the periodic boundary conditions of the method. The Brillouin zone was sampled using a 1×1×25 Monkhorst–Pack k-point grid with a 0.5 shift along each direction. Structural relaxation was also performed through a geometry optimization of 200 steps, using the conjugate gradient method and a force minimization criterion of 0.04 eV/Å between atoms. The displacement step between successive iterations was set to 1.0×10^{-4} Å to avoid large structural distortions and to ensure convergence, considering the asymmetric nature of the chiral CNT edges. The self-consistent field (SCF) calculations were considered converged when the total energy difference between successive iterations was below 1×10^{-4} eV. The method is implemented in the SIESTA software package [**14**], which was employed in this work. After the optimization process, we obtained a diameter and height of approximately 6 Å. The carbon–carbon bond lengths ranged from 1.4 to 1.42 Å, and the bond angles varied between 117° and 120°. **Fig. 1** shows the initial nanotube structure used in this study.

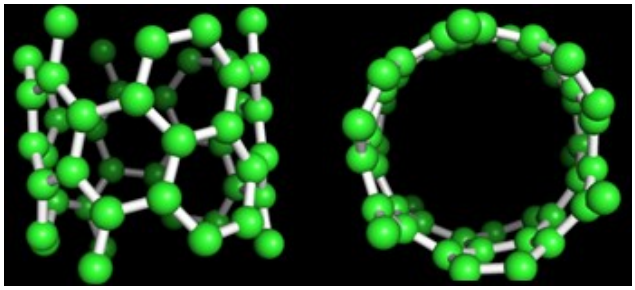

Fig. 1. Primitive model of the Chiral Nanotube CNT - 48 C. Side view (left) and top view (right). Generated in the Pymol program [**15**].

RESULTS AND DISCUSSION

Fig. 2(a) shows the energy band structure of the original CNT–48C unit cell. The Fermi level was centered at the origin for better visualization. The band structure analysis reveals a direct band gap (E_g) of 0.115 eV, indicating near-zero semiconducting behavior, which is consistent with the literature [**4**]. The semiconducting behavior of (6,3) type nanotubes has also been reported in the literature using other computational methodologies [**16-17**].

In **Fig. 2(b)** shows the Density of States (DOS) per electron-volt. The energy scale was centered at the Fermi level for better visualization. A very small separation near the Fermi level can be observed, indicating a semiconducting character close to metallic.

The literature reports that doping CNTs with boron (B) and nitrogen (N) has applications in supercapacitors, gas sensors, blood glucose oxidation, catalysis, and electrocatalysis [**18**]. These potential applications motivated us to dope our CNT-48C model with these elements. The optimization of the B- and N-doped CNTs did not cause any structural distortions, maintaining the original bond angles, bond lengths, and diameters.

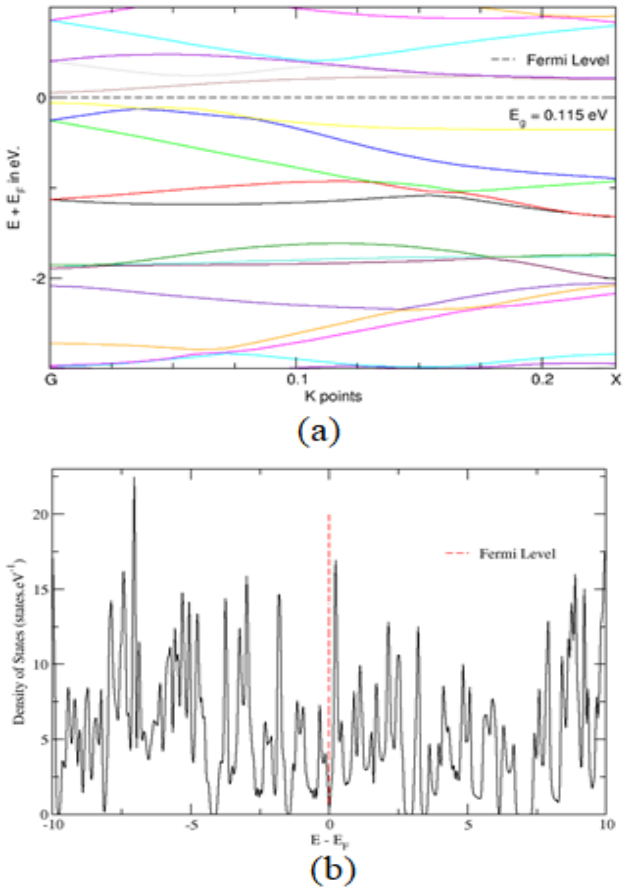

Fig. 2. (a) Energy bands for CNT-48C. The Fermi level has been shifted to zero to facilitate visualization. A direct gap of –0.115 eV around the Fermi level can be observed. (b) Total DOS for CNT-48C with the energies referenced to the Fermi level ($E - E_F$).

In **Fig. 3**, panel (a) shows the nitrogen-doped structure (CNT-47C1N), represented by blue spheres, while panel (b) depicts the energy band structure. The analysis of the band structure reveals an overlap between the valence and conduction bands, indicating metallic behavior, with $E_g = 0$. In panel 3 (c), the total and partial DOS are depicted.

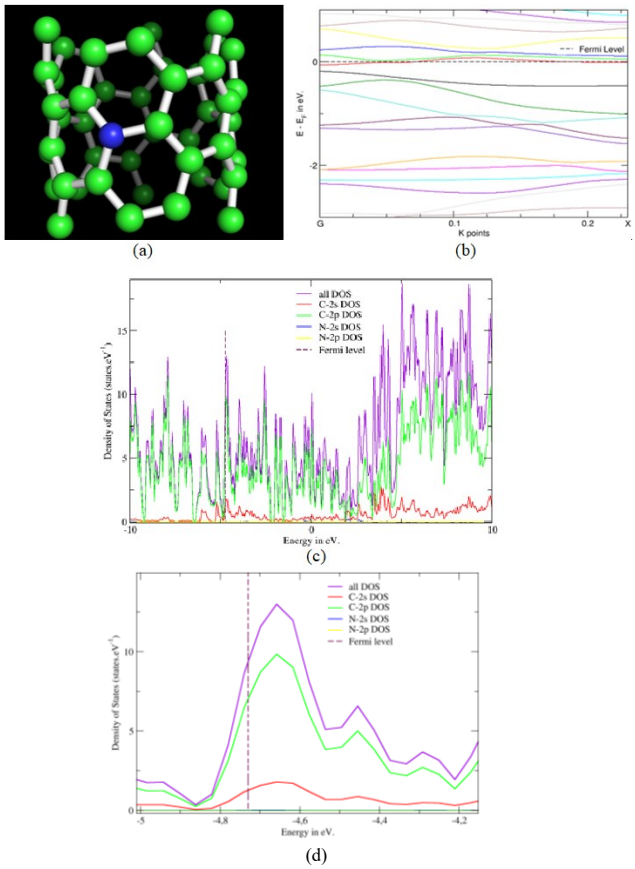

Fig. 3. (a) Nitrogen-doped structure (blue sphere); (b) electronic band structure, where the overlap of the bands around the Fermi level indicates metallic behavior; (c) Total and partial DOS, showing the dominance of C–2p orbitals near the Fermi level; and (d) zoomed-in view of the total and partial DOS near the Fermi level for CNT-47C1N.

The analysis of the DOS shows a higher concentration of carbon 2p orbitals (green line) around the Fermi level compared to the nitrogen 2p orbitals (yellow line), indicating a greater contribution of the carbon 2p orbitals to charge mobility. We integrated the projected density of states (PDOS) near the Fermi level, as shown in **Fig. 3(d)**. The results show that the C–2p orbitals dominate the electronic states, contributing approximately 89% of the total DOS, with minor contributions from C–2s (≈10.8%) and N–2s (≈0.09%), while the N–2p orbitals are negligible. **Fig. 4** shows the results for the carbon nanotube doped with boron (light pink) (CNT-47C1B, panel (a)). In panel (b), the energy band structure of CNT-47C1B shows an overlap of energy bands around the Fermi level, indicating metallic behavior with $E_g = 0$. In panel (c), the total and partial DOS are depicted. Analysis of the DOS, as in the case of CNT-47C1N, shows that the carbon 2p orbitals (red line) are more concentrated around the Fermi level and therefore contribute most significantly to charge mobility. For this case, the results show that the C–2p orbitals dominate the electronic states, contributing approximately 86.6% of the total DOS, with minor contributions from C–2s (≈9.75%) and B–2s (≈0.61%), while the B–2p orbitals contribute about 4.04%. During the fabrication process, carbon vacancies may occur in the nanotube structure, potentially affecting its physical and chemical properties.

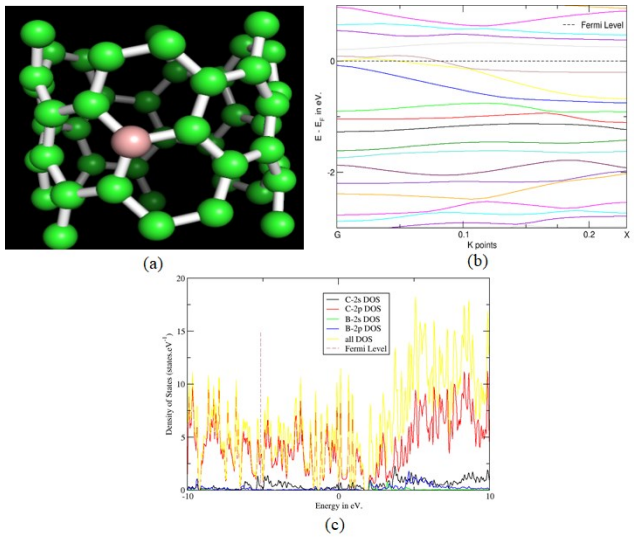

Fig. 4. (a) Boron-doped structure (CNT-47C1B); (b) energy band structure, showing the overlap of energy bands around the Fermi level; and (c) total and partial DOS for CNT-47C1B, showing that the C-2p orbitals dominate the charge-carrier mobility (red line).

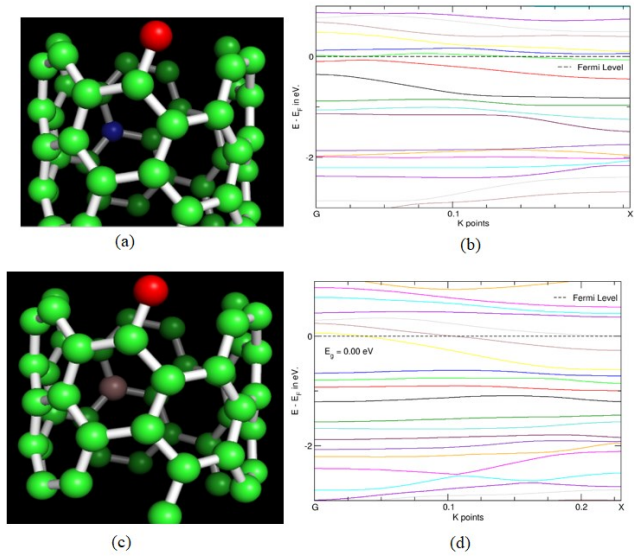

Fig. 5. (a) Nitrogen doping with a single vacancy (CNT-46C1N); (b) energy band structure of CNT-46C1N, indicating metallic behavior; (c) boron doping with a single vacancy (CNT-46C1B); and (d) energy band structure of CNT-46C1B, also exhibiting metallic behavior.

To model such scenarios, **Fig. 5(a)** and **Fig. 5(b)** present the results for CNT-47C1N with a single vacancy (CNT-46C1N), and (c) and (d) show the results for CNT-47C1B with a vacancy (CNT-46C1B). The inclusion of

vacancies did not cause any structural distortions after optimization, preserving the original bond angles, bond lengths, and diameter. The red spheres indicate the positions where a carbon atom was removed (vacancy). In both cases, **Figs. 5** show an overlap of the bands around the Fermi level, indicating $E_g = 0$. We performed a DOS analysis, and the results were similar to those obtained for CNT-47C1N and CNT-47C1B, with a higher concentration of carbon 2p orbitals around the Fermi level, thus contributing most significantly to charge mobility. **Fig. 6** presents the DOS for CNT-46C1B.

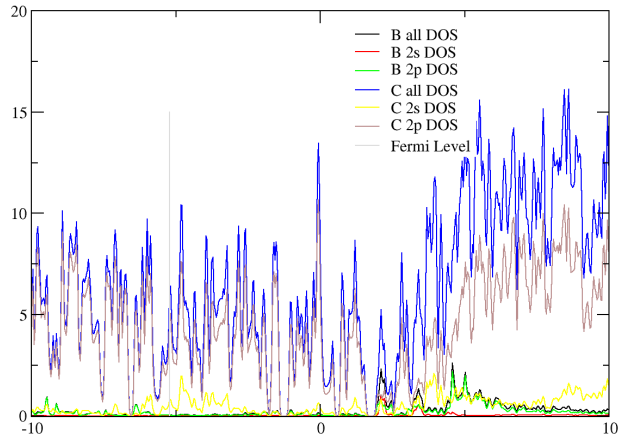

Figu. 6. Total and partial DOS (vertical axis) as a function of energy (horizontal axis), centered at the Fermi level (gray line) for CNT-46C1B, indicating that the C-2p orbitals (brown line) dominate the charge mobility.

The partial contributions to the density of states near the Fermi level for this case were practically identical to those observed for CNT-47C1B, with the following percentages: C–2p = 87.6%, C–2s = 9.97%, B–2s = 0.61%, and B–2p = 4.02%.

Finally, the metallic character increases the electrical conductivity of the nanotube due to the enhanced electronic mobility near the Fermi level. Low resistivity is an important feature for supercapacitor electrodes, as it contributes to reducing the internal resistance and thus improves the energy release performance (increased power density) [**19**]. For sensor applications, the semiconducting behavior is more advantageous due to its higher capability to detect molecules or gases [**20**].

CONCLUSION

Carbon nanotubes are nanomaterials with significant technological applications across various industries. Their uses range from batteries to pharmaceuticals, among others. In this work, we present a study using Density Functional Theory (DFT) on chiral carbon nanotubes of type (6,3). Our model consisted of 48 carbon atoms, with a diameter and height of approximately 6 Å. After optimizing the structure using the Siesta program, the carbon-carbon distances ranged from 1.4 to 1.42 Å, and the carbon-carbon bond angles varied between 117° and 120°. The analysis of our results led to the following conclusions:

1. Chiral (6,3) carbon nanotubes are semiconductors with a small band gap. The energy band analysis revealed a nearly zero direct band gap of 0.115 eV, which aligns with values reported in the literature.
2. Substitutional doping with nitrogen (N) and boron (B) atoms resulted in an overlap of the valence and conduction bands around the Fermi level, indicating metallic behavior.
3. The inclusion of vacancies in the doped structures did not affect the metallic behavior, maintaining a null band gap.
4. Chemical analysis showed that, for all cases investigated, there was a higher concentration of carbon atom 2p states around the Fermi level, suggesting that these states contribute most significantly to charge mobility.
5. For supercapacitor applications, metallic behavior is more suitable for nanotube-based electrodes. In contrast, for gas sensor applications, semiconducting behavior is more appropriate.

ACKNOWLEDGEMENTS

We would like to thank the Federal Institute of Espírito Santo, Brazil, for their support and encouragement.

CONFLICTS OF INTEREST

There are no conflicts to declare.

REFERENCES

1. Oliveira, I.; De Jesus, V. L. B.; Introduction to Solid State Physics (3 ed.); Physics Bookstore, São Paulo, **2017**.
2. Day, L.; Mau, A. W. H.; *Adv. Mater*. **2001**, 13, 899. https://doi.org/10.1002/1521-4095(200107)13:12/13<899::AID-ADMA899>3.0.CO;2-G.
3. Saito, R.; Dresselhaus, G; Dresselhaus, M. S.; Physical Properties of Carbon Nanotubes, Imperial College Press, London, **1998**.
4. Filho, A. G. de S.; Fagan, S. B.; *Química Nova*, **2007,** 30, 7. https://doi.org/10.1590/S0100-40422007000700037.
5. Leite, C. F.; Study of Electrons and Phonons in Carbon Nanotubes through Resonant Raman Scattering - Thesis (PhD); Department of Physics - Federal University of Minas Gerais, Belo Horizonte - Brazil, **2005**.
6. Yang, Q. H.; Hou, P. X.; Unno, M.; Yamauchi, S.; Saito, R.; Kyotani T., *Nano Lett*., **2005**, 5, 2465–2469. https://doi.org/10.1021/nl051779j.
7. Bulusheva, L. G.; Fedorovskaya, E. O.; Kurenya, A. G.; Okotrub, A. V.; *Phys. Status Solidi* B, **2013**, 250, 2586–2591. https://doi.org/10.1002/pssb.201300108.
8. Ghosh, K.; Kumar, M.; Maruyama, T.; Ando, Y.; *Carbon*, **2009**, 47, 1565–1575. https://doi.org/10.1016/j.carbon.2009.02.007.
9. Salazar, P. F.; Kumar, S.; Cola, B. A. J.; *Electrochem. Soc*., **2012**, 159, B483–B488. https://doi.org/10.1149/2.043205jes.
10. Nanotube modeler - Program for generating xyz-coordinates for Nanotubes and Nanocones. Available in: http://www.jcrystal.com/products/wincnt/. Accessed 04 April **2025**.
11. Pseudopotential Virtual Vault. Available in: https://nninc.cnf.cornell.edu/periodic_table.html. Accessed 04 april **2025**.
12. De Oliveira, P. J. P.; De Jesus, L. G.; Jekel, D. C.; De Souza, M. R.; Castelan Marques, F.; *Nanomaterials Science & Engineering*, **2024**, 6, 27-37. https://doi.org/10.34624/nmse.v6i1.35515.

13. Castillo, M. S.; *Carbon Nanotube Conditioning: Ab Initio Simulations of the Effect of Interwall Interaction, Defects and Doping on the Electronic Properties of Carbon Nanotubes*; Dissertation (Doctor of Philosophy), Rice University, Houston, USA, **2017**. Available in: https://repository.rice.edu/items/d178fc74-1a7c-420f-9fbe-e2800a85ef6b. Accessed 11 november **2025.**
14. Soler, J. M.; Artacho, E.; Gale, J. D.; Garcia, A.; Junquera, J.; Ordejón, P.; Sánchez-Portal, D.; *Phys. Cond. Matt*., **2002**, 14, 2745. https://doi.org/10.1088/0953-8984/14/11/302.
15. Pymol. Available in: https://pymol.org/. Accessed 04 april 2025.
16. Dehbandi, B.; Zardoost, M. R.; Mirjafary, Z.; Hossaini, Z.; *Journal of Molecular Structure*, **2020,** 1205, 127662. https://doi.org/10.1016/j.molstruc.2019.127662.
17. Zardoost, M. R.; Dehbandi, B.; *Physica E*, **2013**, 54, 226. http://dx.doi.org/10.1016/j.physe.2013.06.024.
18. Yan, Y.; Miao, J.; Yang, Z.; Xiao, F.; Yang, H. B.; Liu, B.; Yang, Y.; *Chem. Soc. Rev*., **2015**, 44, 3295. https://doi.org/10.1039/c4cs00492b.
19. Pan, H.; Li, J.; Feng, Y. P.; *Nanoscale Res. Lett.*, **2010**, 5, 654. https://doi.org/10.1007/s11671-009-9508-2.
20. Schroeder, V.; Savagatrup, S.; He, M.; Lin, S.; Swager, T. M.; *Chem. Rev*., **2019**, 119, 599–663. https://doi.org/10.1021/acs.chemrev.8b00340.

AUTHORS BIOGRAPHY

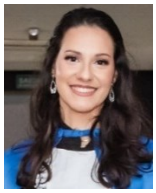

Thaizy C. Nossa holds a degree in Physics (2023) and a technical diploma in Biotechnology (2017), both from the Federal Institute of Education, Science and Technology of Espírito Santo (IFES), Brazil. She is currently pursuing a Master's degree in Science with an emphasis on Materials Physics at the Federal University of Ouro Preto (UFOP), Brazil, which she began in 2024. Her research focuses on carbon nanotubes, with material characterization performed through Raman spectroscopy.

Professor Paulo completed his Ph.D. in Atomic and Molecular Physics at the Federal University of Espírito Santo, Brazil, in 2010. He is currently a professor at the Federal Institute of Espírito Santo, Cachoeiro de Itapemirim campus, where he conducts research projects and supervises students in the fields of nanoscience and physics education.

GRAPHICAL ABSTRACT

Synopsis: Chiral carbon nanotube with Hamala indices (6,3) and graphs of energy bands and total and partial density of states, indicating semiconducting behavior close to metallic, with a band gap of 0.115 eV.